



HAL
open science

Lagged effect of the Pacific Decadal Oscillation on decadal variation in global land precipitation

Lili Liang, Shijing Liang, Laurent Z X Li, Huiling Yuan, Zhenzhong Zeng

► **To cite this version:**

Lili Liang, Shijing Liang, Laurent Z X Li, Huiling Yuan, Zhenzhong Zeng. Lagged effect of the Pacific Decadal Oscillation on decadal variation in global land precipitation. *The Innovation Geoscience*, 2023, 1 (3), pp.100034. 10.59717/j.xinn-geo.2023.100034 . hal-04786768

HAL Id: hal-04786768

<https://hal.science/hal-04786768v1>

Submitted on 16 Nov 2024

HAL is a multi-disciplinary open access archive for the deposit and dissemination of scientific research documents, whether they are published or not. The documents may come from teaching and research institutions in France or abroad, or from public or private research centers.

L'archive ouverte pluridisciplinaire **HAL**, est destinée au dépôt et à la diffusion de documents scientifiques de niveau recherche, publiés ou non, émanant des établissements d'enseignement et de recherche français ou étrangers, des laboratoires publics ou privés.



Distributed under a Creative Commons Attribution - NonCommercial - NoDerivatives 4.0 International License



Lagged effect of the Pacific Decadal Oscillation on decadal variation in global land precipitation

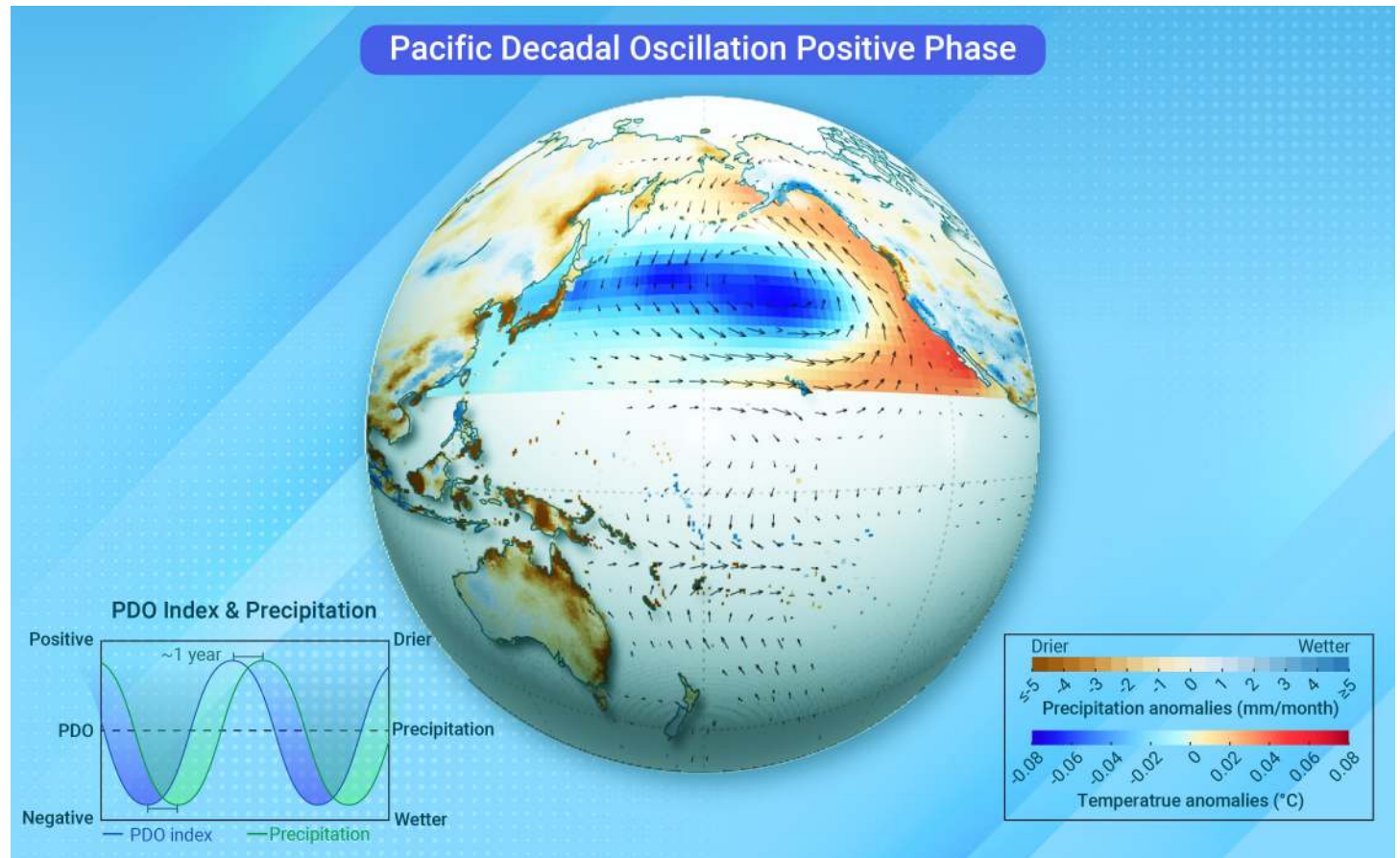
Lili Liang,¹ Shijing Liang,¹ Laurent Z. X. Li,² Huiling Yuan,³ and Zhenzhong Zeng^{1,*}

*Correspondence: zengzz@sustech.edu.cn (Z.Z.)

Received: July 19, 2023; Accepted: November 8, 2023; Published Online: November 15, 2023; <https://doi.org/10.59717/j.xinn-geo.2023.100034>

© 2023 The Author(s). This is an open access article under the CC BY-NC-ND license (<http://creativecommons.org/licenses/by-nc-nd/4.0/>).

GRAPHICAL ABSTRACT



PUBLIC SUMMARY

- The response of global land precipitation to the Pacific Decadal Oscillation (PDO) is delayed by about one year.
- Positive PDO phases have a stronger effect on precipitation changes.
- PDO in each season tends to influence land precipitation in the following season.
- The lag is driven by the PDO persistent influence on the atmospheric circulation.



Lagged effect of the Pacific Decadal Oscillation on decadal variation in global land precipitation

Lili Liang,¹ Shijing Liang,¹ Laurent Z. X. Li,² Huiling Yuan,³ and Zhenzhong Zeng^{1,*}

¹School of Environmental Science and Engineering, Southern University of Science and Technology, Shenzhen 518055, China

²Laboratoire de Météorologie Dynamique, CNRS, Sorbonne Université, École Normale Supérieure, École Polytechnique, Paris 75005, France

³School of Atmospheric Sciences, Nanjing University, Nanjing 210023, China

*Correspondence: zengzz@sustech.edu.cn (Z.Z.)

Received: July 19, 2023; Accepted: November 8, 2023; Published Online: November 15, 2023; <https://doi.org/10.59717/j.xinn-geo.2023.100034>

© 2023 The Author(s). This is an open access article under the CC BY-NC-ND license (<http://creativecommons.org/licenses/by-nc-nd/4.0/>).

Citation: Liang L., Liang S., Li L., et al., (2023). Lagged effect of the Pacific Decadal Oscillation on decadal variation in global land precipitation. *The Innovation Geoscience* **1**(3), 100034.

The Pacific Decadal Oscillation (PDO), as the leading mode of sea surface temperature (SST) in the North Pacific, modulates the global temperature and precipitation. While previous studies have shown a negative relationship between the global precipitation and the PDO, the time-delayed feature of this relationship remains underexplored. Here we investigate the lagged effect of the decadal variations in the PDO on the global land precipitation using cross-correlation at multiple scales. We find that there is a delayed response of precipitation to the PDO, with the regional correlation peaking at a certain delay and gradually decreasing with increasing lag time. We note the asymmetric impacts of the positive and negative PDO phases on precipitation. Seasonal analysis reveals that the PDO is related to land precipitation during the subsequent season relative to the rest of the year, with the highest correlation occurring in the boreal winter. The delay in response is likely due to the constant SST forcing of the PDO to the atmospheric circulation. This study highlights the lag duration of the PDO–precipitation relationship, potentially enriching our understanding of this relationship and enhancing climate predictions on decadal timescales.

INTRODUCTION

Oceanic modes are significant factors in shaping climate patterns, with their influence on precipitation constituting a topic of ongoing research.^{1–3} These oceanic modes, such as the El Niño–Southern Oscillation (ENSO), Atlantic Multidecadal Oscillation (AMO), and Pacific Decadal Oscillation (PDO), intricately link ocean–atmosphere processes. They modulate the heat distribution, atmospheric circulation, and moisture transport, subsequently influencing precipitation.^{1,4–6} Amidst the ENSO phase shift from La Niña to El Niño in 2023, it appears that the PDO may undergo phase alterations with potential far-reaching changes in precipitation, building upon previously studied decadal-scale connections with precipitation dynamics.^{7,8}

As global precipitation is influenced by diverse factors such as solar radiance,^{9,10} aerosols,^{2,11,12} and climate change,^{13–16} this complicates the identification of the impact of the PDO on precipitation. Previous studies have met this challenge by focusing on specific regional patterns,^{17–19} analyzing different PDO phases,¹ and utilizing advanced statistical methods.²⁰ For instance, Duan et al.²¹ highlighted the significant influence of the PDO on precipitation in southern China. Dai²² explored the connection between the Interdecadal Pacific Oscillation (IPO, a comparable oceanic mode to the PDO) and precipitation in the U.S., providing insights into regional effects. Dong and Dai¹ extended the above exploration by examining the influence of the IPO on precipitation and temperature, offering a global perspective and regional connections during the positive and negative PDO phases. Furthermore, researchers have explored different aspects of precipitation, including droughts and extremes,^{8,23} which might be related to the PDO. Some researchers have suggested that the PDO may interact with other climate modes, such as the ENSO, to jointly influence precipitation patterns.^{8,24,25} For instance, Ouyang et al.¹⁹ investigated the signal and combined impact of the ENSO and PDO on precipitation and stream flow in China. Nalley et al.²⁶ using a wavelet-based method, presented a multiscale analysis of the individual and combined influences of the PDO, ENSO, and North Atlantic Oscillation (NAO) on precipitation in watersheds.

However, despite the valuable insights provided in previous studies, the potential time delay in the relationship between the PDO and precipitation has not been extensively explored. Considering how the PDO modulates the

regional precipitation variability, particularly in areas bordering the Pacific Ocean and extending to other regions through teleconnections, it is plausible to consider that these processes occur with time lags. In this study, we comprehensively analyze the lagged correlation between the PDO and precipitation, examining global and regional scales, as well as seasonal and interseasonal variations. This study aims to contribute to the growing understanding of the PDO–precipitation relationship and enhance climate predictions on decadal timescales.

DATA AND METHODS

In this study, PDO time series data were sourced from the NOAA Physical Sciences Laboratory, derived from the NOAA Extended Reconstructed SST V5 (ERSST V5) dataset.²⁷ The PDO index (PDOI) represents the leading principal component time series obtained through the application of empirical orthogonal function (EOF) analysis to sea surface temperature anomalies in the North Pacific region (20°–70° N, 110° E–100° W). The monthly global precipitation used for analysis was obtained from the Climatic Research Unit time series version 4.06 (CRU TS v.4.06).²⁸ This dataset has been instrumental in understanding the various aspects of climate variability and changes over the past century since 1900 with a spatial resolution of 0.5° × 0.5°. ²⁹ Our study period coincides with the data range, spanning from 1901 to 2021. To enhance robustness, we used additional precipitation datasets, including the precipitation reconstruction over land (PRECL) product of the U.S. Climate Prediction Center and datasets of the Global Precipitation Climatology Centre (GPCC)³⁰ and the University of Delaware (UDEL).³¹ Furthermore, we incorporated monthly surface pressure and 100-m wind speed data from the ERA5 reanalysis dataset³² and NINO3.4 data from the NOAA.³³ By combining these datasets, we aimed to explore the complex interplay between the PDO and precipitation patterns and uncover the underlying mechanisms that drive these relationships.

To investigate the relationship between the PDO and land precipitation, we first derived the decadal changes in both variables. We applied a Butterworth filter³⁴ with a 10-year cutoff to extract the decadal fluctuations in the PDO index. Similarly, regarding precipitation, we removed the monthly climatology and applied a 10-year low-pass filter. We then obtained the decadal variations in land precipitation by removing the linear trend in the study period (1901–2021) from the 10-year low-pass data, minimizing the impact of other factors, such as aerosols on decadal precipitation variations.

With the decadal changes in the PDO and precipitation obtained, we employed a cross-correlation function of these variables. This function is effective in revealing the delay time between two variables by measuring their similarity while one is time-shifted, allowing us to pinpoint the time lag when the correlation between the PDO and precipitation is strongest.³⁵ To supplement cross-correlation analysis, we assessed the reliability of the correlation coefficients (r) by determining whether significant differences existed between the delayed and instantaneous correlations. Additionally, we used the information flow tool,^{36,37} a method for quantifying the rate at which information flows from one sequence to another, thus confirming the potential causal relationships between the PDO and land precipitation. These approaches should contribute to our understanding of the lagged relationship between the PDO and land precipitation.

RESULTS

Global correlation of the PDO and land precipitation

In general, lower (higher) precipitation anomalies are associated with the

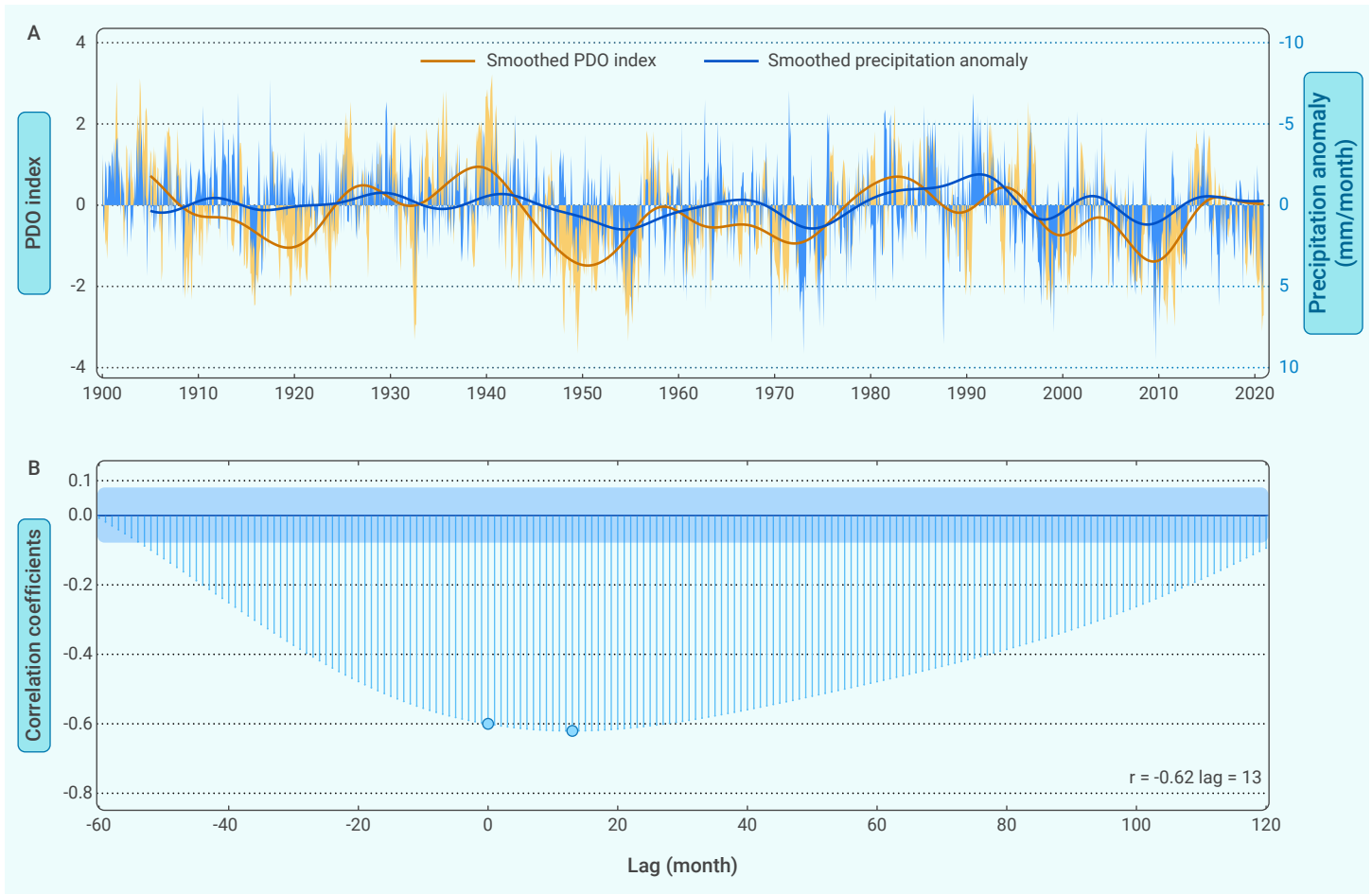


Figure 1. Decadal variation in global mean precipitation over land and cross-correlation function with PDO index from 1901 to 2021 (A) Time series of PDO index (PDOI) and precipitation anomaly (shading in yellow and blue) and their 10-year cutoff lowpass series. (B) The cross-correlation function of smoothed PDOI and precipitation anomaly. That 1391 degrees of freedom available yield a 95% confidence level of 0.08 (blue band; more details refer to supplemental methods). The two outlined points are respectively correlation coefficients (r) at lag 0 and the highest at a positive lag (PDO changes lead those of precipitation).

positive (negative) PDO phase (Figure 1). As an example, from the late 1940s to the 1950s, when the PDO occurred in a negative phase, the precipitation anomalies were high. Figure 1B shows the relationship between the correlation coefficient (r) and the lag in which the r value increases with increasing lag of the PDO leading to rainfall, peaking at 15 months (with $r = -0.56$). Then, as the lag time increases beyond the optimal delay, the relationship slowly weakens. This suggests that there exists a delayed response between the PDO and precipitation, with PDO changes leading to variations in precipitation. To substantiate our findings, we extended the analysis to the GPCC, PRECL, and UDEL datasets, which similarly displayed delayed correlations with the PDO (Figure S1). This consistency confirms that the observed lags are not simply due to random chance but instead indicates a meaningful association between the two variables.

As the PDO is the leading mode of SSTs in the North Pacific and oscillates between positive and negative phases, this climate cycle affects the temperature and precipitation patterns throughout the Pacific basin and beyond.¹ Figure 2 shows the correlation pattern at region-specific time delays (Figure S2). Notably, the r value differences resulting from these delays are significantly less than 0 (Figure S3), amplifying the negative PDO–precipitation correlation.

Since the sign of the correlation exhibits inconsistency globally, we focused our analysis on six regions, each characterized by relatively high correlation, as outlined in Figure 2A. Most regions exhibit a negative correlation between the PDO and precipitation. Western North America is an exception (Figure 2F), indicating a positive relationship likely influenced by PDO-related wind patterns transporting moisture to the region, as supported by atmospheric dynamics (Figure S4). Furthermore, we found significant information flow from the PDOI to the decadal precipitation series in all outlined regions except

South America. This suggests a potential absence of a causal linkage between the two variables in parts of South America, despite the high correlation coefficients. Moreover, in regions distant from the North Pacific (e.g., parts of Europe and Inner Asia), where precipitation is more likely controlled by the Arctic Oscillation, polar vortex and Siberian high pressure,^{38,39} the nature of precipitation varies on (inter)annual or shorter timescales. This leads to a weaker decadal signal and nonsignificant, fragmented correlation coefficients.

Asymmetric influence of the PDO on precipitation

Consistent with the correlation pattern, positive and negative precipitation anomalies are observed during the positive and negative PDO phases (Figure 3), highlighting the substantial influence of the PDO on the precipitation distribution. During the positive PDO phases, less precipitation is expected across large areas of the tropics relative to historical averages, and slightly higher than average precipitation is observed in parts of the U.S. (Figure 3A). During the negative phase of the PDO, the opposite pattern typically arises (Figure 3B). Notably, the absolute magnitude of the average precipitation anomalies is larger during the positive PDO phases than during the negative PDO phases, possibly attributed to the combined influence of PDO-related dynamics and the superimposed impact of the ENSO during the positive PDO phases.^{8,25}

While atmospheric pressure systems and wind patterns tend to be symmetric during the positive and negative PDO phases (Figure S4), the irregular distribution of landmasses and ocean basins can channel and modify moisture transport in a nonuniform and asymmetric manner.^{40,41} In certain regions, moisture convergence during the negative PDO phases can enhance rainfall, whereas during the positive phases, the altered processes

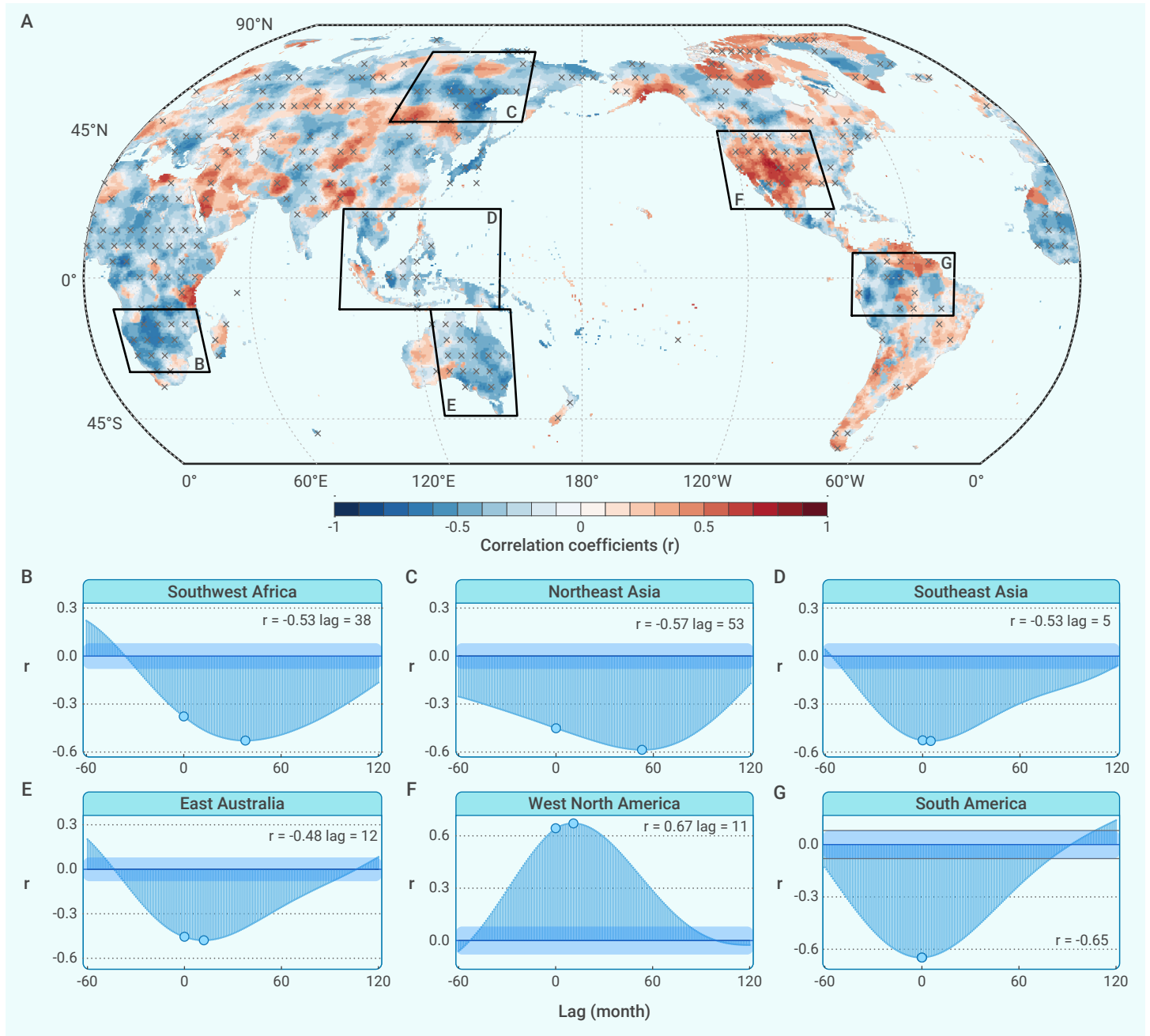


Figure 2. Cross-correlation between local smoothed precipitation anomaly and PDOI (A) Shading shows the cross-correlation coefficients (r) at maximal absolute with positive lags (0 included). The unshaded area has nonsignificant r ($p < 0.05$). Areas with cross show the significant information flow from the PDOI to precipitation. The corresponding lag duration to the r value refers to Figure S2. (B-G) The cross-correlation function of smoothed PDOI and precipitation anomaly over different regions. The regions delineated by black boxes in Figure 2A were considered, and within each box, calculations were performed solely for the dominant correlation sign area. The two blue points are respectively correlation coefficients at lag 0 and the highest at a positive lag (PDO changes lead those of precipitation). In South American (G), the maximal correlation is at lag of 0.

may yield a stronger drying effect (Figure S5). Additionally, El Niño/La Niña events introduce an extra layer of dry/wet influence on precipitation patterns. Specifically, La Niña events interact with the negative PDO phase, possibly resulting in increased precipitation and partially counterbalancing the asymmetric patterns (Figures S5 and S6). Collectively, these factors contribute to the observed asymmetry in the impact of the PDO on precipitation.

Seasonally lagged correlation between the PDO and precipitation

While operating on a decadal scale, investigating the seasonal effects of the PDO remains crucial for comprehending its impact on seasonal precipitation patterns. This extended analysis aims to contribute to a greater understanding of how PDO impacts are distributed within a year and to enhance our capacity to predict accurate climatic trends. Figure 4 shows the cross-correlation of the PDO and precipitation during each season. The overall

correlation in December-January-February (DJF) is higher than that during the other seasons, with the following order: September-October-November (SON), June-July-August (JJA), and March-April-May (MAM). The areas with significant r values follow a different order, i.e., DJF, MAM, SON, and JJA, with the only consistency indicating that boreal winter is the season with the strongest linkage.^{1,3,42}

In terms of the spatial distribution, the DJF patterns exhibit a closer resemblance to the global monthly correlations than those during the other seasons (Figures 2A and 4A), suggesting that PDO-related precipitation anomalies are mainly prevalent during the DJF season. Substantial precipitation anomalies during the positive/negative PDO periods in DJF support this speculation (Figures S7 and S8). Moreover, for inland regions of Eurasia and Africa, during the MAM season, the PDO shows smaller areas with a significant precipitation correlation relative to DJF, and this correlation decreases in JJA. Such a

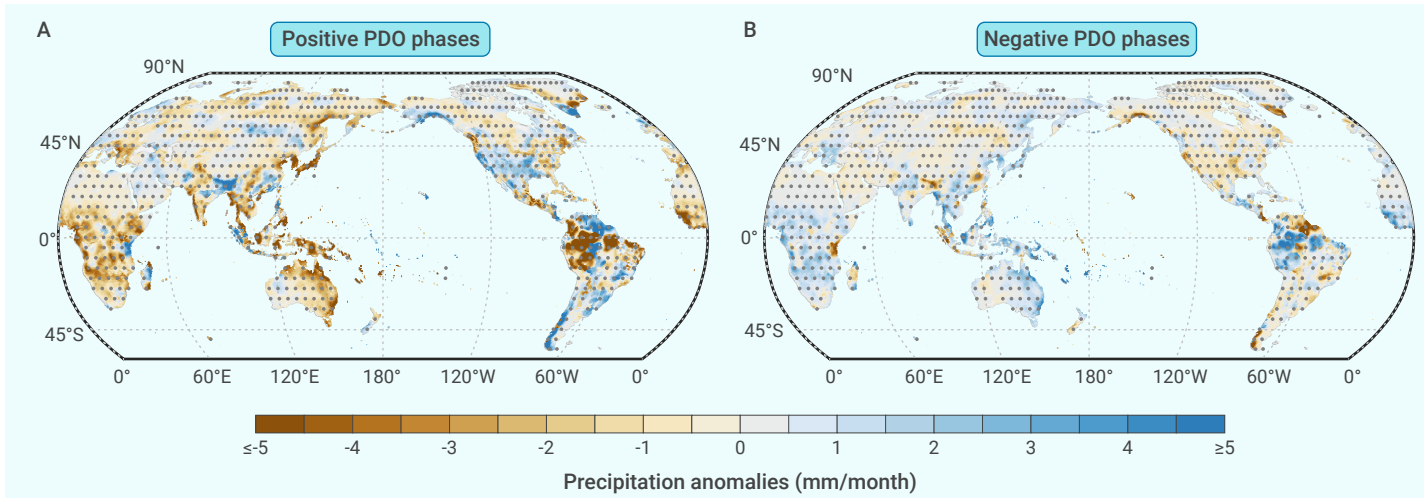


Figure 3. Spatial patterns of lagged precipitation anomalies over land at different PDO phases from 1901-2021 (A) Average of lagged precipitation anomalies when smoothed $PDOl > 0$, and (B) when $PDOl < 0$. Note that the anomalies are obtained from the PDO phases with local time lag (Figure S2). The dots show that the mean precipitation anomalies are significantly different from the mean from 1901 to 2021 at a 95% confidence level using a two-tailed *t*-test.

seasonal development of the correlation coefficient prompts us to wonder whether, in addition to the same-season correlation, there may be a delayed correlation between the PDO and precipitation between seasons.

We then analyzed the cross-correlation between the PDO and precipitation across the four seasons using yearly averaged series (Table 1). Our findings revealed that, except for the boreal winter, the precipitation during each season is more closely tied to the PDO state during the preceding season rather than during the same season (Table 1). For instance, the boreal summer (JJA) precipitation exhibits a more pronounced relationship with the PDO in the boreal spring (MAM) relative to the other seasons ($r = -0.53$, lag = 0). It is important to note that a lag value of 0 in the table indicates that there is no year-time delay, but a season-time delay still exists when the data originate from different seasons. This points to a potential delayed impact of the PDO in spring on the following summer precipitation patterns. The relationship is consistent for the boreal summer PDO and autumn precipitation. The mechanism behind this seasonal lag effect could be the relatively timely atmospheric responses. During PDO transition from MAM to JJA, atmospheric conditions, such as surface pressure and jet stream patterns, may well be integrated into MAM PDO states that allow the influence to be transmitted to the JJA precipitation.

In contrast, for lags exceeding 0, such as the MAM precipitation influenced by the DJF PDO from 5 years prior ($r = -0.49$, lag = 5), our hypothesis underscores the impact of evolving PDO conditions, particularly prominent in DJF,^{4,22} on MAM precipitation patterns. Given the extended evolution of oceanic anomalies of the PDO, the delayed response likely arises from the time needed for ocean-atmosphere interactions to fully shape precipitation patterns. Although specific lag values might not precisely reflect actual years of the lagged process, they offer directional insights and help identify potential connections.

To more comprehensively investigate the mechanism underlying the observed correlations, we examined the large-scale atmospheric circulation patterns associated with the PDO by regressing surface pressure and wind speed anomalies onto the PDO index. These patterns offer a snapshot of the simultaneous atmosphere response to the PDO, constituting an integral component of the complex interactions responsible for precipitation anomalies. The DJF pattern resembles the overall regression pattern more than the JJA pattern in the North Pacific (Figures 5A and S4), reinforcing the heightened PDO influence in the boreal winter.¹⁴ The low pressure and wind pattern in the North Pacific in DJF explains the positive correlation in the western US: the prevailing winds and low-pressure systems tend to favor increased moisture transport into the western U.S., resulting in higher precipitation levels.^{1,23} This agrees with the findings of Dong et al.⁴³ for the deepened Aleutian low and extended westerly jet stream driving increased precipitation in California during the positive IPO phase. Conversely, during the negative PDO phases, these atmospheric conditions tend to shift, leading to reduced moisture

transport and lower precipitation levels in the same area.

In contrast, the climate pattern in JJA exhibits slight symmetry along the equator relative to that in DJF, as indicated by the presence of a low-pressure system over the South Pacific (Figure 5B). This variance in climate patterns partially accounts for the DJF PDO not consistently exhibiting the highest correlation with precipitation across all seasons, despite its pronounced influence in DJF.⁴ As the PDO-related climatic patterns change with the season, the mechanisms that contribute to upcoming precipitation anomalies are set in motion. Consequently, the seasonal connection of precipitation with the preceding PDO state is notably stronger (Table 1).

DISCUSSION

While our previous discussion revealed correlations across the different seasons, the nature of the PDO as a driver of mid- to high-latitude sea surface temperature anomalies should be considered the factor shaping the lagging precipitation. In contrast to the tropics, where the ocean primarily drives atmospheric changes, the middle and high latitudes often experience atmospheric forcing on the ocean.^{44,45} The ocean functions as an integrator, gradually converting random atmospheric fluctuations into more persistent sea surface temperature anomalies.⁴⁶ When the sustained anomalies form a certain SST pattern, they will in turn set in motion processes for the redistribution of heat and moisture in the atmosphere.^{41,47} This includes the modulation of large-scale atmospheric circulation patterns and precipitation patterns. The delayed effect arises from the time needed for these processes to propagate and interact across different regions. As a result, we observe varying time delays between the PDO phase and subsequent precipitation changes across different areas. Understanding this time-delayed effect is crucial for accurately predicting and understanding regional climate variations associated with the PDO. Notably, other factors within the climate system, such as vegetation,^{48,49} ENSO,³⁰ or climatic anomalies stemming from other regions, such as the Arctic Oscillation,⁵¹ may also contribute to this lag. The interplay among these various factors further adds complexity to our understanding of the teleconnections between the PDO and global precipitation anomalies.

The observed larger precipitation anomalies during the positive PDO phases than during the negative phases can be primarily attributed to the systematic distinction of PDO-induced atmospheric circulation distribution patterns. When investigating potential reasons, it becomes important to consider the influences of El Niño and La Niña events during the positive/negative PDO phases on precipitation, which also appears to exhibit asymmetry but does not alter our conclusions (Figures 3 and S6). Several studies have revealed complex interactions between the ENSO and PDO and their impact on precipitation patterns.^{8,25} For instance, Roy¹⁷ and Xiao et al.⁵² found that the ENSO and PDO can jointly lead to more pronounced precipitation anomalies in certain regions in India and China, respectively. There are

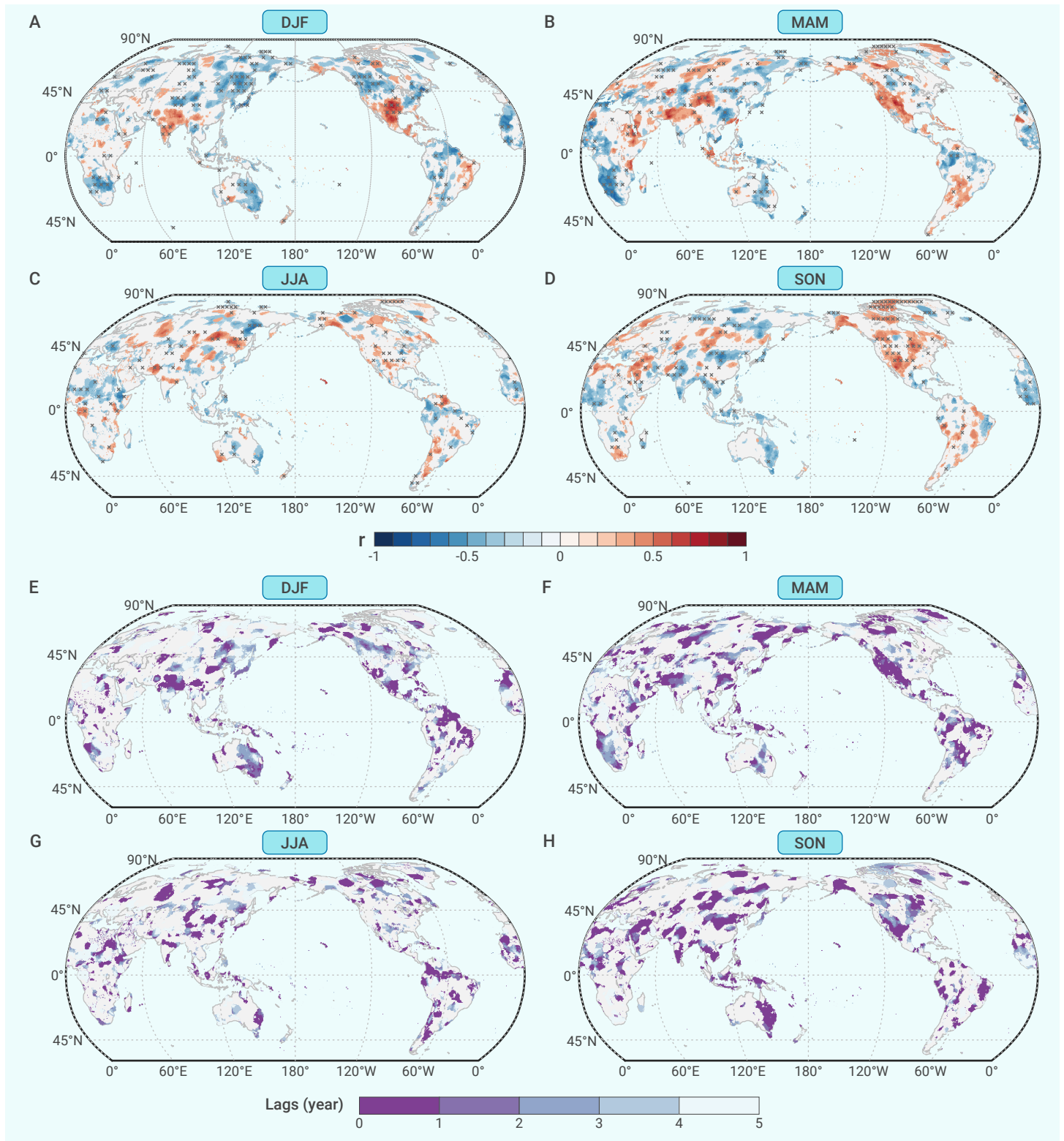


Figure 4. Seasonal cross-correlation between local smoothed precipitation anomaly and PDOI (A)-(D) Shading shows the cross-correlation coefficients (r) at maximal absolute with positive lags (0 included), respectively for December-February (DJF), March-May (MAM), June-August (JJA), and September-November (SON). And 115 degrees of freedom available yield a 95% confidence level of 0.28. The unshaded area has nonsignificant r . Areas with cross show the significant information flow from the PDOI to precipitation. (E)-(H) The lag duration respectively corresponds to the r in (A)-(H).

also studies providing evidence that ENSO events impose asymmetric influences on the stratospheric polar vortex intensity during the different PDO phases.⁵³ Based on our findings, this may warrant further investigation. Our analysis suggested that the presence of ENSO events could influence precipitation anomalies, even though we removed the high-frequency component of precipitation.

Finally, our findings should be interpreted within the context of an evolving climate system. While our study primarily focused on the relationship between the PDO and precipitation, it is important to recognize climate change and its potential influence on precipitation trends. Numerous studies have highlighted the impact of climate change on precipitation patterns, including increased occurrences of extreme precipitation events, shifts in

Table 1. The relationship between precipitation and the PDO across different seasons.

Precipitation	PDO			
	DJF	MAM	JJA	SON
DJF	-0.62 (3)	-0.58 (2)	-0.47 (1)	-0.47 (3)
MAM	-0.49 (5)	-0.39 (4)	-0.44 (4)	-0.44 (5)
JJA	-0.51 (0)	-0.53 (0)	-0.47 (0)	-0.44 (0)
SON	-0.36 (0)	-0.52 (0)	-0.56 (0)	-0.52 (0)

Note: December-January-February (DJF) refers to the average of December of the previous year and the first two months of the current year. MAM, JJA, and SON are respectively abbreviations for March-April-May, June-July-August, and September-October-November. The correlation coefficient with the largest absolute value in the positive lag period is presented. Degrees of freedom (115) available yield a 95% confidence level of 0.28. In parentheses is the corresponding lag period (in years).

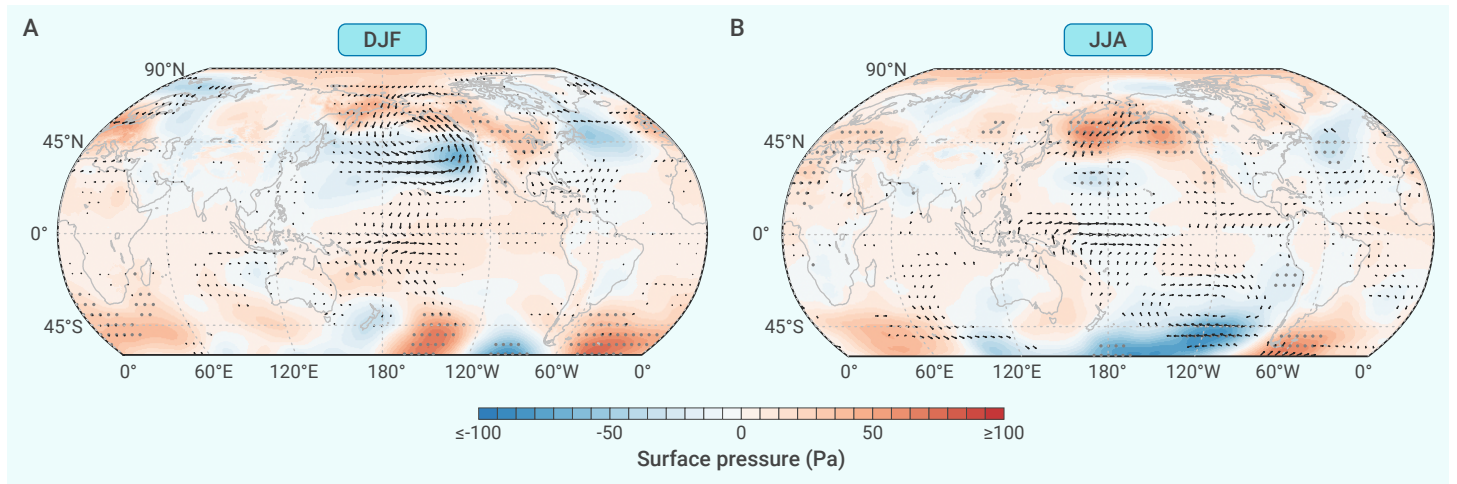


Figure 5. Spatial pattern of surface pressure and 100-m wind speed based on PDOI in DJF and JJA (A) Simultaneous regression patterns of surface pressure (Pa; shading areas) and wind speed (m/s; arrows) based on PDOI in DJF. The dots show the significance at a 95% confidence level and only the significant wind pattern is present. (B) Same as (A), but for JJA. The numbers below the color bar indicate the pressure change for the unit PDOI change.

regional precipitation patterns, and modifications in the overall water cycle.⁵⁴⁻⁵⁶ These alterations could interact with PDO-driven variations, potentially complicating the interpretation of our results. To mitigate the potential effects of long-term climate change trends and other factors, we removed the linear trend from the precipitation data. Despite the simplified method, our study offers insight into the complex interplay between decadal oceanic modes in shaping precipitation patterns across regions and timescales.

CONCLUSION

In this study, we established a significant lagged correlation between the PDO and global precipitation over land, with cross-correlation analysis revealing that precipitation anomalies are likely to fluctuate following PDO changes. We observed that regionally, the western U.S. exhibits positive correlations with the PDO, while many other areas worldwide, including northeastern Siberia, Australia, and vast regions in the tropics, show negative correlations. Positive PDO phases tend to induce drier conditions relative to the dampening influence associated with the negative PDO phases. When examining the relationship seasonally, the PDO exhibits the strongest correlation with precipitation during the boreal winter and tends to show a better correlation with precipitation in the next month, offering a predictive potential for upcoming precipitation events. This study underlines the importance of considering both the lag time and correlation coefficient when investigating the relationship between the PDO and precipitation, which could be useful for improving precipitation simulations and predictions.

REFERENCES

- Dong, B., and Dai, A. (2015). The influence of the Interdecadal Pacific Oscillation on Temperature and Precipitation over the Globe. *Clim. Dyn.* **45**, 2667–2681.
- Gu, G., Adler, R.F., and Huffman, G.J. (2015). Long-term changes/trends in surface temperature and precipitation during the satellite era (1979–2012). *Clim. Dyn.* **46**, 1091–1105.
- Hu, Z.Z., Kumar, A., Jha, B., and Huang, B. (2019). How much of monthly mean precipitation variability over global land is associated with SST anomalies. *Clim. Dyn.* **54**, 701–712.
- Newman, M., Alexander, A.M., Ault, R.T., et al. (2016). The Pacific Decadal Oscillation, revisited. *J. Clim.* **29**, 160310134237003.
- Rasmusson, E.M., and Arkin, P.A. (1993). A global view of large-scale precipitation variability. *J. Clim.* **6**, 1495–1522.
- Knight, J.R., Folland, C.K., and Scaife, A.A. (2006). Climate impacts of the Atlantic Multidecadal Oscillation. *Geophys. Res. Lett.* **33**, L17706.
- Kwon, M., Yeh, S.W., Park, Y.G., and Lee, Y.K. (2013). Changes in the linear relationship of ENSO–PDO under the global warming. *Int. J. Climatol.* **33**, 1121–1128.
- Nguyen, P.L., Min, S.K., and Kim, Y.H. (2020). Combined impacts of the El Niño–Southern Oscillation and Pacific Decadal Oscillation on global droughts assessed using the standardized precipitation evapotranspiration index. *Int. J. Climatol.* **41**, E1645–E1662.
- Xue, J., Ning, L., Liu, Z., et al. (2022). The combined influences of solar radiation and PDO on precipitation over eastern China during the last millennium. *Clim. Dyn.* **60**, 1137–1150.
- Lambert, F.H., Stott, P.A., Allen, M.R., and Palmer, M.A. (2004). Detection and attribution of changes in 20th century land precipitation. *Geophys. Res. Lett.* **31**, L10203.
- Shen, T., Sun, W., Liu, J., et al. (2022). Secular changes of the decadal relationship between the northern hemisphere land monsoon rainfall and sea surface temperature over the past millennium in climate model simulations. *J. Geophys. Res. Atmos.* **127**, e2022JD037065.
- Iles, C.E., Hegerl, G.C., Schurer, A.P., and Zhang, X. (2013). The effect of volcanic eruptions on global precipitation. *J. Geophys. Res. Atmos.* **118**, 8770–8786.
- Lambert, F.H., Stine, A.R., Krakauer, N.Y., and Chiang, J.C.H. (2008). How much will precipitation increase with global warming. *Eos. Trans. A.G.U.* **89**, 193–194.
- Jalilhal, C., Srinivasan, J., and Chakraborty, A. (2020). Different precipitation response over land and ocean to orbital and greenhouse gas forcing. *Sci. Rep.* **10**, 11891.
- Previdi, M., and Liepert, B.G. (2008). Interdecadal variability of rainfall on a warming planet. *Eos. Trans. A.G.U.* **89**, 193–195.

16. Marvel, K., and Bonfils, C. (2013). Identifying external influences on global precipitation. *Proc. Natl. Acad. Sci. U.S.A.* **110**, 19301–19306.
17. Roy, S.S. (2013). The impacts of ENSO, PDO, and local SSTs on winter precipitation in India. *Phys. Geogr.* **27**, 464–474.
18. Yao, J., Xiao, L., Gou, M., et al. (2018). Pacific decadal oscillation impact on East China precipitation and its imprint in new geological documents. *Sci. China Earth Sci.* **61**, 473–482.
19. Ouyang, R., Liu, W., Fu, C., et al. (2014). Linkages between ENSO/PDO signals and precipitation, streamflow in China during the last 100 years. *Hydrol. Earth Syst. Sci.* **18**, 3651–3661.
20. Ekhtiari, N., Agarwal, A., Marwan, N., and Donner, R.V. (2019). Disentangling the multi-scale effects of sea-surface temperatures on global precipitation: A coupled networks approach. *Chaos* **29**, 063116.
21. Duan, W., Song, L., Li, Y., and Mao, J. (2013). Modulation of PDO on the predictability of the interannual variability of early summer rainfall over south China. *J. Geophys. Res. Atmos.* **118**, 13,008–13,021.
22. Dai, A. (2013). The influence of the inter-decadal Pacific oscillation on US precipitation during 1923–2010. *Clim. Dyn.* **41**, 633–646.
23. Wei, W., Yan, Z., and Li, Z. (2021). Influence of Pacific Decadal Oscillation on global precipitation extremes. *Environ. Res. Lett.* **16**, 044031.
24. Pierce, D.W., DeFlorio, M.J., Cayan, D.R., and Miller, A.J. (2013). Western U.S. extreme precipitation events and their relation to ENSO and PDO in CCSM4. *J. Clim.* **26**, 4231–4243.
25. Lee, S.-H., Seo, K.-H., and Kwon, M. (2019). Combined effects of El Niño and the Pacific Decadal Oscillation on summertime circulation over east Asia. *Asia-Pacific J. Atmos. Sci.* **55**, 91–99.
26. Nalley, D., Adamowski, J., Biswas, A., et al. (2019). A multiscale and multivariate analysis of precipitation and streamflow variability in relation to ENSO, NAO and PDO. *J. Hydrol.* **574**, 288–307.
27. Huang, B., Thorne, W.P., Banzon, F.V., et al. (2017). Extended reconstructed sea surface temperature, Version 5 (ERSSTv5): upgrades, validations, and intercomparisons. *J. Clim.* **30**, 8179–8205.
28. Harris, I., Osborn, T.J., Jones, P., and Lister, D. (2020). Version 4 of the CRU TS monthly high-resolution gridded multivariate climate dataset. *Sci. Data* **7**, 109.
29. Sun, Q., Miao, Q., Ashouri, D. h., et al. (2018). A review of global precipitation data sets: data sources, estimation, and intercomparisons. *Rev. Geophys.* **56**, 79–107.
30. Schneider, U., Hånsel, S., Finger, P., et al. (2022). GPCC full data monthly product version 2022 at 0.5°: Monthly Land-Surface Precipitation from Rain-Gauges built on GTS-based and Historical Data. 10.5676/DWD_GPCC/FD_MLV2022_050.
31. Legates, D. R., and Willmott, C. J. (1990). Mean seasonal and spatial variability in gauge-corrected, global precipitation. *Int. J. Climatol.* **10**, 111–127.
32. Hersbach, H., Bell, B., Berrisford, P., et al. (2020). The ERA5 global reanalysis. *Q. J. R. Meteorol. Soc.* **146**, 1999–2049.
33. Rayner, N.A., Parker, D.E., Horton, E.B., et al. (2003). Global analyses of sea surface temperature, sea ice, and night marine air temperature since the late nineteenth century. *J. Geophys. Res.* **108**, 4407.
34. Butterworth, S. (1930). On the theory of filter amplifiers. *Wirel. Eng.* **7**, 536–541.
35. Wilson, G.T. (2016). *Time series analysis: forecasting and control*, 5th Edition, by George E. P. Box, Gwilym M. Jenkins, Gregory C. Reinsel and Greta M. Ljung, 2015. Published by John Wiley and Sons Inc., Hoboken, New Jersey, pp. 712. ISBN: 978-1-118-67502-1. *J. Time Ser. Anal.* **37**, 709–711.
36. Liang, X.S. (2014). Unraveling the cause-effect relation between time series. *Phys. Rev. E* **90**, 052150.
37. Liang, X.S. (2015). Normalizing the causality between time series. *Phys. Rev. E* **92**, 022126.
38. He, S., Gao, Y., Li, F., et al. (2017). Impact of Arctic Oscillation on the east Asian climate: A review. *Earth Sci. Rev.* **164**, 48–62.
39. Zhang, J., Zheng, H., Xu, M., et al. (2022). Impacts of stratospheric polar vortex changes on wintertime precipitation over the northern hemisphere. *Clim. Dyn.* **58**, 3155–3171.
40. Gimeno, L., Dominguez, F., Nieto, R., et al. (2016). Major mechanisms of atmospheric moisture transport and their role in extreme precipitation events. *Annu. Rev. Environ. Resour.* **47**, 117–141.
41. Leduc, G., Vidal, L., Tachikawa, K., et al. (2007). Moisture transport across Central America as a positive feedback on abrupt climatic changes. *Nature* **445**, 908–911.
42. Yang, X., and Huang, P. (2022). Improvements in the relationship between tropical precipitation and sea surface temperature from CMIP5 to CMIP6. *Clim. Dyn.* **60**, 3319–3337.
43. Dong, L., Leung, L.R., Song, F., and Lu, J. (2021). Uncertainty in El Niño-like warming and California precipitation changes linked by the Interdecadal Pacific Oscillation. *Nat. Commun.* **12**, 6484.
44. Seager, R., and Murtugudde, R. (1997). Ocean dynamics, thermocline adjustment, and regulation of tropical SST. *J. Clim.* **10**, 521–534.
45. Sasaki, H., Klein, P., Qiu, B., and Sasai, Y. (2014). Impact of oceanic-scale interactions on the seasonal modulation of ocean dynamics by the atmosphere. *Nat. Commun.* **5**, 5636.
46. Di Lorenzo, E., and Ohman, M. D. (2013). A double-integration hypothesis to explain ocean ecosystem response to climate forcing. *Proc. Natl. Acad. Sci. U.S.A.* **110**, 2496–2499.
47. England, M.H., McGregor, S., Spence, P., et al. (2014). Recent intensification of wind-driven circulation in the Pacific and the ongoing warming hiatus. *Nat. Clim. Chang.* **4**, 222–227.
48. Li, Y., Piao, S., Li, L.Z.X., et al. (2018). Divergent hydrological response to large-scale afforestation and vegetation greening in China. *Sci. Adv.* **4**, eaar4182.
49. Sikma, M., and Vilà-Guerau de Arellano, J. (2019). Substantial reductions in cloud cover and moisture transport by dynamic plant responses. *Geophys. Res. Lett.* **46**, 1870–1878.
50. Wu, X., and Mao, J. (2016). Interdecadal modulation of ENSO-related spring rainfall over South China by the Pacific Decadal Oscillation. *Clim. Dyn.* **47**, 3203–3220.
51. Wang, J., and Ikeda, M. (2000). Arctic oscillation and Arctic sea-ice oscillation. *Geophys. Res. Lett.* **27**, 1287–1290.
52. Xiao, M., Zhang, Q., and Singh, V.P. (2015). Influences of ENSO, NAO, IOD and PDO on seasonal precipitation regimes in the Yangtze River basin, China. *Int. J. Climatol.* **35**, 3556–3567.
53. Sobaeva, D., Zyuilyaeva, Y., and Gulev, S. (2023). ENSO and PDO effect on stratospheric dynamics in Isca numerical experiments. *Atmosphere* **14**, 459.
54. Estrada, F., Kim, D., and Perron, P. (2021). Spatial variations in the warming trend and the transition to more severe weather in midlatitudes. *Sci. Rep.* **11**, 145.
55. Pendergrass, A.G., Knutti, R., Lehner, F., et al. (2017). Precipitation variability increases in a warmer climate. *Sci. Rep.* **7**, 17966.
56. Routson, C.C., McKay N., Kaufman D., et al. (2019). Mid-latitude net precipitation decreased with Arctic warming during the Holocene. *Nature* **568**, 83–87.

ACKNOWLEDGMENTS

This research is funded by the National Natural Science Foundation of China, grant no. 42071022 (NSFC), and Start-up Fund provided by Southern University of Science and Technology, no. 29/Y01296122 (SUSTech). This study was supported by Center for Computational Science and Engineering at Southern University of Science and Technology. We thank any individuals or organizations who contributed to the datasets and methods used in this study.

AUTHOR CONTRIBUTIONS

Zhenzhong Zeng provided the conception, funding acquisition, and supervision. Lili Liang conducted the investigation, visualization, methodology and wrote the original manuscript. Shijing Liang contributed to the editing of the manuscript. Laurent Z. X. Li and Huiling Yuan contributed to the interpretation of the results.

DECLARATION OF INTERESTS

The authors declare no competing interests.

SUPPLEMENTAL INFORMATION

It can be found online at <https://doi.org/10.59717/j.xinn-geo.2023.100034>

LEAD CONTACT WEBSITE

<https://www.zhenzhongzeng.com/>